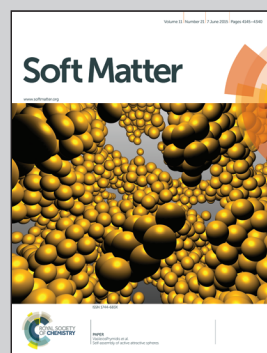


Highlighting work from T. Galstian's Research Group, Université Laval, Québec, Canada.

Molecular self-assemblies might discriminate the diffusion of chiral molecules

How chiral molecules propagate in self aligned elastic molecular complexes where the microscopic diffusion process is coupled with macroscopic boundary conditions of the host medium creating thus molecular orientation quantization zones (with different colorations); a phenomenon, the understanding of which might improve the drug delivery or chiral discrimination processes.

### As featured in:



See Tigran Galstian and Karen Allahverdyan,  
*Soft Matter*, 2015, **11**, 4167.



Cite this: *Soft Matter*, 2015,  
11, 4167

Received 2nd January 2015,  
Accepted 10th April 2015

DOI: 10.1039/c4sm02904f

[www.rsc.org/softmatter](http://www.rsc.org/softmatter)

## Molecular self-assemblies might discriminate the diffusion of chiral molecules

Tigran Galstian\* and Karen Allahverdyan

Biological tissue has many self-aligned anisotropic molecular organizations, which are able to undergo reversible orientational deformations and spatially transfer them. At the same time, the majority of drugs and many biologically important molecules contain chiral centers. It is therefore important to understand the factors affecting the diffusion of chiral molecules in such elastic environments. We experimentally study the diffusion of chiral molecules in a nematic liquid crystal host representing the model of biological tissue. The analogy of Cano's quantization effect is observed (due to the gradient of the chiral dopant) and used to estimate the corresponding diffusion coefficients. It is shown that thanks to the collective orientational correlation of host molecules the diffusion of chiral dopants is noticeably reduced (by a factor of  $\approx 1.6$ ) for the case of rigid alignment of host molecules compared to the case when the same matrix is free to adjust that alignment.

Almost half of the drugs currently in use are chiral compounds, the majority of which is racemic (equimolar mixture of two enantiomers).<sup>1</sup> The control of their delivery and release in the human body is thus very important<sup>2,3</sup> since the better understanding of the diffusion and aggregation of those molecules (once released in the tissue) may help to optimize their impact. Those diffusion processes are mainly studied in isotropic environments, but the molecular diffusion in anisotropic media is also well known.<sup>4</sup> In reality however, the physical environment (the biological tissue), where chiral molecules usually diffuse, is very often not only anisotropic, but also elastic. Elasticity here stands for the capacity of the host to undergo reversible orientational deformations of its collective molecular alignment and to transfer that deformation in space, for example, as it is the case in liquid crystals (LC).<sup>5</sup> Examples of such natural self-assembled structures in the biological world are numerous, from cell membranes and myelin to aligned collagen fibers<sup>6</sup> and fibrillar aggregates of amyloid plaques.<sup>7</sup> This similarity has triggered the use of LC materials as tissue models to study the light transport in such media.<sup>8</sup> The transport and behavior of molecules,<sup>9,10</sup> colloidal micro-particles<sup>11</sup> and biological micro-objects, such as bacteria,<sup>12–17</sup> were also studied in such elastic anisotropic media. However, to the best of our knowledge, the impact of host's elasticity and, most importantly, of its orientational boundary conditions on

the diffusion of chiral molecules has not yet been reported in the literature.

In the present work we show experimentally that the elasticity and the boundary conditions (imposed on the collective molecular orientation) of the host medium play an important discriminating role in the diffusion dynamics of chiral molecules. This phenomenon must thus be taken into account in applications involving their diffusion, for example, when designing chiral drugs for the treatment of specific diseases in molecular self-aligned environments.

To demonstrate the above-mentioned phenomenon, we have used nematic liquid crystal (NLC) pentylcyanobiphenyl (5CB) that is in the LC phase (its molecules are naturally aligned in the same direction, called *director* and represented by a unit vector  $\mathbf{n}$ )<sup>5</sup> at room temperature. The 5CB was acquired from Sigma-Aldrich and injected into a sandwich-like structure composed of two 0.5 mm thick glass substrates, each of them being spin-coated (internal sides only) by a thin (50 nm) layer of polyimide (PI), from Nissan. The role of PI was to promote planar (tangential) alignment of the director on the surfaces of both substrates. In one part of our experiments those PI layers were used without mechanical rubbing, which resulted in planar alignment of the NLC's director  $\mathbf{n}$  without preferential alignment in the substrate's plane X, Y<sup>18</sup> (Fig. 1). In the second part of our experiments, standard "antiparallel" (along +X and -X directions) mechanical rubbing of the PI was performed (before the assembly of the final sandwich) to impose a "strongly" preferred planar alignment along the X axis, (Fig. 1). To prevent the NLC from leaking out of the sandwich, the periphery of the "bottom" substrate (positioned with its PI layer facing "up") was covered by UV curable adhesive walls

Center for Optics, Photonics and Lasers, Department of Physics, Engineering Physics and Optics, Laval University, Pav. d'Optique-Photonique, 2375 Rue de la Terrasse, Québec, Canada G1V 0A6. E-mail: galstian@phy.ulaval.ca, karen.allaahverdyan.1@ulaval.ca; Tel: +1-418-6562025

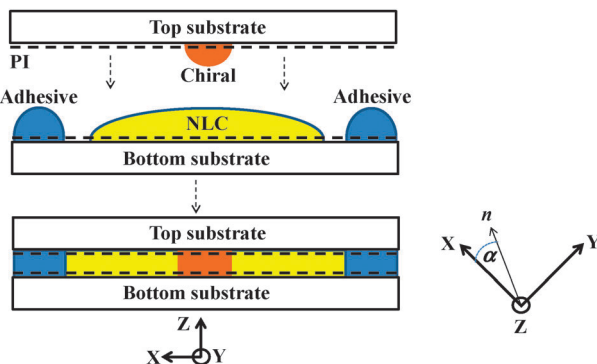


**Fig. 1** Schematic demonstration of the fabrication technique of the liquid crystal sandwich (left) with the insertion of the droplet of chiral liquid. The dashed horizontal lines represent the PI layers. Vertical dashed arrows show the process flow. The right inset shows the deviation (at angle  $\alpha$ ) of the director's orientation from the preferential direction  $X$ .

(NOA 65, in the form of a ring of  $\phi \approx 3$  cm) containing glass spacers (diameter  $\phi \approx 8 \mu\text{m}$ ) to provide the desired thickness of the NLC layer (top left, Fig. 1). The thickness of the NLC cell was measured in different positions (particularly around the zone of analyzes, see hereafter) to insure its uniformity within  $\pm 0.2 \mu\text{m}$  (thanks to the very thick glass substrates used).

The drop of NLC was injected inside the reservoir created by those walls. In the case of standard NLC sandwiches, the second “top” (identical) substrate is usually pressed (with the PI layer facing “down”) on the drop of the NLC and the peripheral adhesive is cured by a UV lamp (with spectra between 300–450 nm, intensity of  $\approx 10 \text{ mW cm}^{-2}$ , irradiation time  $\leq 10$  min, exposition at room temperature  $T = 22^\circ\text{C}$ , with particular attention to avoid heating) while protecting the central part of the cell by a UV-blocking mask. In this case, well known uniformly aligned (mono-domain) NLC sandwiches are obtained when using rubbed PI layers. Chaotically aligned (while still in the  $X$ ,  $Y$  plane) multi-domain layers are obtained in the opposite case (no PI rubbing).

In the case reported in the current work, we have added another step in the fabrication of sandwiches. Namely, a small droplet (with a diameter of  $\phi \approx 2$  mm, see top left, Fig. 1) of a liquid composed of chiral molecules (*R,R*) 1-phenyl-1,2-bis[4-(*trans*-4-pentylcyclohexylbenzenecarbonyl)]ethane (purchased from AWAT) was dispensed on the PI layer of the top substrate before joining the two substrates as described above (the bottom substrate bearing the large droplet of NLC and the top substrate with the small droplet of the chiral liquid, maintained by surface tension forces). A small liquid zone (with chiral molecules) is thus obtained that is surrounded by the 5CB (left bottom, Fig. 1).

Fabricated samples were inserted into a Zeiss polarizing microscope and their images (observed through crossed polarizers) were recorded at different times by a photographic system for the same position and orientation of the sample. Typical examples of obtained pictures (of the “dark” chiral liquid surrounded by “colored” 5CB) are presented in Fig. 2 for two cases of sandwiches, fabricated with rubbed (top line, noted as “Rubbed (strong)”) and

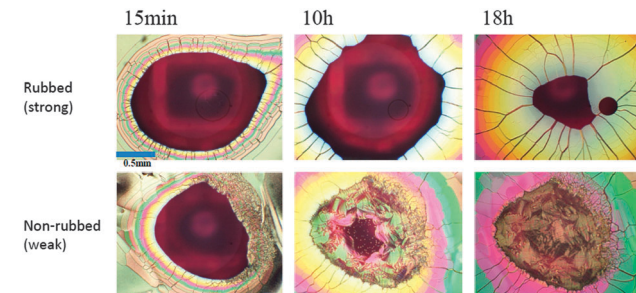


**Fig. 2** Examples of pictures, recorded at different times (15 min, 10 h and 18 h) in the polarizing microscope (crossed polarizers), for the sandwiches fabricated with rubbed (top line) and non-rubbed (bottom line) layers of PI. The small horizontal bar (in the top left picture) shows 0.5 mm length.

non-rubbed (bottom line, noted as “Non-rubbed (weak)”) PI layers. Times (15 min, 10 h and 18 h), when those pictures were recorded, are shown on the top of each column. As we can see, in the case when the PI layers were rubbed (top line, Fig. 2), the central part of the droplet of the chiral liquid remains un-dissolved even after 18 hours (top right picture, Fig. 2). At the same time, we observe almost complete inter-diffusion of chiral and 5CB molecules in the case of non-rubbed sandwiches (bottom right picture, Fig. 2). A closer look on the boundary of the chiral droplet with 5CB (see the top left picture of Fig. 2) shows that clearly distinguishable zones are formed parallel to that boundary (Fig. 3a). The widths (noted as  $d$ ) of those zones grow with time (Fig. 3b) and thus their frontiers (the distance from the chiral droplet’s border, noted as  $r$ ) also move (Fig. 3c) with respect to the center of the chiral droplet. We can also notice (Fig. 2 and 3b) that the “evolution” of those zones is different in the cases of sandwiches with rubbed and non-rubbed PI (noticeably faster growth for non-rubbed PI).

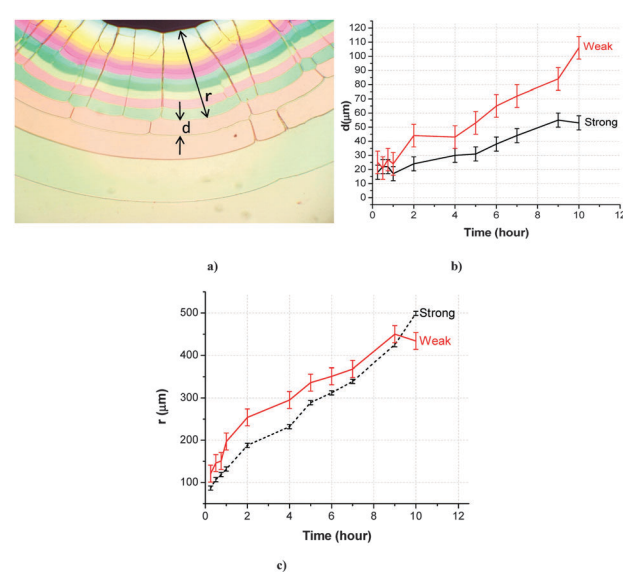


**Fig. 3** (a) Zoom on the top left picture of Fig. 2; (b) temporal evolution of the width  $d$  of one discrete zone, (c) temporal evolution of the position  $r$  of the same zone. Different positions of the given zone (for the cases of rubbed, “strong” and non-rubbed, “weak”, PI layers) were analyzed to generate enough statistics and the corresponding error bars.

## Discussion

It is well known<sup>5</sup> that, in the absence of chiral dopants or in the case of racemic equilibrium, the rubbing of PI<sup>18</sup> allows obtaining well-aligned uniform layers of NLC (see hereafter), corresponding to the minimum free energy density of the material system. The left side of Fig. 4 schematically demonstrates (noted as “Nematic zone  $n + 2$ ”) such uniformly aligned NLC molecules (filled ellipses). However, the condition of minimum free energy in the presence of chiral dopants corresponds to the helical rotation of the director  $\mathbf{n}$  around the  $Z$  axis<sup>5</sup> (Fig. 4), with its  $X$  and  $Y$  components, defined as  $n_x = \cos \theta(z)$ ,  $n_y = \sin \theta(z)$  and  $\theta = q_0 z = (2\pi/\Lambda_0)z$ , the  $\Lambda_0$  being the complete ( $360^\circ$ ) rotation period of  $\mathbf{n}$ . Given that standard NLCs are locally reciprocal (directions  $+\mathbf{n}$  and  $-\mathbf{n}$  are equivalent), the periodicity  $P_0$  of material properties will be observed at the half of the complete rotation period  $\Lambda_0$  ( $P_0 = \Lambda_0/2$ ). Furthermore, in cases where there are no strong orientational boundary conditions, the “free” period of the system  $P_f$  is defined, among other parameters, by the concentration  $C$  of chiral molecules (in addition to the specificities of the solute–solvent pair, the temperature, etc.<sup>5,9</sup>). In contrast, if the LC layer is confined in an environment where the boundary conditions are fixed (for example, the rubbed PI layers are forcing  $\mathbf{n}$  to be aligned in the direction of  $X$  axis at both internal surfaces of substrates,  $z = 0$  and  $z = L$ , Fig. 4), then the alignment distribution  $\mathbf{n}(z)$  of the entire cluster must be adjusted (by slightly changing its rotation period  $P \neq P_f$ ) to minimize the bulk orientational elastic deformation energy density  $W_D$  of the system.<sup>5</sup> Indeed, in this case, the director's reorientation on the surface (say at an angle  $\alpha$  from the preferential orientation direction  $X$ , see the right inset of Fig. 1) will require overpassing the in-plane (or azimuthal) anchoring energy  $W_A(\alpha) \propto \sin^2 \alpha$ .<sup>19</sup> Thus, as far as the  $W_D$ , related to the above-mentioned period (or pitch) adjustment, is less than  $W_A$  (which is typically the case with the rubbed PI), a “quantization” of director's rotation happens (to maintain  $\mathbf{n}(z = 0) \parallel \mathbf{n}(z = L) \parallel X$ )

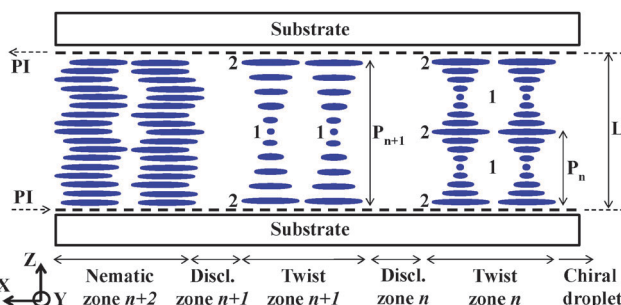


Fig. 4 Schematic demonstration of various slices of the LC layer with uniformly aligned nematic cluster (on the extreme left, Nematic zone “ $n + 2$ ”) and of two differently twisted zones (Twist zones “ $n + 1$ ” and “ $n$ ”) of LC clusters (with different half periods  $P$  of the director's rotation along the  $Z$  axis), which are separated by disclination zones (Discl. zones “ $n + 1$ ” and “ $n$ ”). The rubbing directions of PI layers (dashed lines) are shown by opposed horizontal dashed arrows on the left. The concentration of the chiral dopant is higher in the extreme right corner (chiral droplet). Points 1 correspond to positions where the director is almost perpendicular to the drawing plane, while this direction is almost parallel to the rubbing directions in points 2 (including on top and bottom substrates).

by producing an integer number of rotation half-periods along the  $Z$  axis:  $P = L/m$ , where  $L$  is the thickness of the LC layer and  $m$  is an integer ( $m = 0, 1, 2, 3, \dots$ ). This quantization phenomenon was studied by Cano<sup>5,20</sup> in the case when a constant concentration of chiral dopants ( $C = \text{const}$ ) was present in the LC, but the sandwich had mutually tilted substrates forming thus a wedge (the thickness  $L$  of the LC layer was gradually changing in the  $X$  direction; not shown in the Fig. 4).

We think that our observations (Fig. 3a) may be considered as the analogy of Cano's quantization effect, but in the case of parallel substrates ( $L = \text{const}$ ) and non-uniform concentration  $C(x)$  of the chiral dopant. Indeed, the contact of the liquid chiral droplet with the NLC layer generates a concentration gradient along the  $X$  axis *via* anisotropic diffusion (see hereafter). Consequently, thanks to the non-zero helical twisting power  $\beta$  of the chiral dopant, the LC must adopt twisted state.<sup>5,9</sup> However, the director's rotation angle (at  $z = 0$  and  $z = L$ ) cannot gradually follow the dopant's concentration in the case of sandwiches with rubbed PI, which corresponds to *strong* boundary conditions ( $W_A \gg W_D$ ). Thus, the extreme left corner of Fig. 4 schematically represents the NLC cluster (Nematic zone  $n + 2$ ) where the concentration  $C(x)$  of chiral molecules is below the threshold required to generate one half-period of molecular rotation. Consequently, all LC molecules here are parallel to the  $X$  axis. The middle zone of Fig. 4 (named “Twist zone  $n + 1$ ”) schematically shows the case when  $C$  is high enough to generate director's rotation on  $\approx 180^\circ$  (with the half period of  $P_{n+1}$  equal to the thickness  $L$  of the LC layer). The next zone (named “Twist zone  $n$ ”) has higher  $C$  (compared to its left neighboring zone) that is high enough to produce an additional half-period of rotation (so a total of  $\approx 360^\circ$ ), obviously with a twice smaller period ( $P_n = P_{n+1}/2$ ). Those zones are typically separated by areas of abrupt changes of the director's orientation (so-called disclination zones,<sup>5</sup> see *Discl. zones “ $n$ ” and “ $n + 1$ ”* in Fig. 4). Thus, we think that the colored parallel zones (with distinct boundaries), observed in our experiment (Fig. 3a), are LC clusters with various pitches  $P$  (each consecutive zone has an additional half rotation period) and those zones are separated by narrow (dark) disclination zones. Different colors of those zones are conditioned by the chromatic dispersion of the rotation of probe light's polarization. Indeed, it is well known that the twisted LC layers may rotate light's polarization at an angle  $\Psi$  that depends, among other parameters, upon the wavelength of light  $\lambda_0$  and the spatial rotation period  $P$  of the director.<sup>5</sup> This rotation may be described by de Vries's or Oseen's formalism.<sup>21,22</sup> We have to note that a meniscus effect (interface curvature along the  $Z$  axis) might also exist at the boundaries between different zones (particularly, between the NLC host and the drop of the chiral dopant). However we observe uniform colored zones with widths  $d \geq 100 \mu\text{m}$ , which excludes the possibility of having those menisci to be responsible for coloration of such large zones (in an NLC cell of  $L = 8 \mu\text{m}$  thickness).

Thus, the frontiers of colored zones (the width “ $d$ ” of each zone, confined between closest disclination zones) correspond to the concentration difference  $\Delta C = C(x_n) - C(x_{n+1})$  that is high

enough to generate enough additional twisting force (of the LC's director) that would energetically justify the creation of a pitch jump<sup>5,20,23</sup> compared to the  $W_D$  that would be required to further adjust the pitch without the jump. In reality, we should also add to this energetic consideration the energy of disclination walls.<sup>5,24</sup> Obviously this argumentation is valid in the case of strong boundary condition (rubbed PI) providing anchoring energy  $W_A$  that is high enough to impose those jumps. In the case of weak azimuthal alignment (PIs' are not rubbed), the in-plane reorientation of the director requires less energy and, consequently, the requirement of quantization of its rotation is much weaker (the director's alignments at  $z = 0$  and  $z = L$  may be changed with the concentration gradient of the chiral dopant).

While we realize that the twisting force, elastic energy and the diffusion, observed here, are rather complicated processes, for the sake of approximate estimations, we can consider an inverse linear dependence of the twist period  $P$  upon the propagation (diffusion) of the chiral dopant (that is appropriate for dilute solutions<sup>5,9</sup>) as

$$P \approx \frac{1}{\beta \gamma \nu}$$

where  $\gamma$  is the enantiomeric excess ( $\gamma = 1$  in the present case) and  $\nu$  is the solute molar fraction.

Let us note that in a well-aligned mono-domain NLC, the diffusion of molecules along the direction of  $\mathbf{n}$  and in the plane that is perpendicular to  $\mathbf{n}$  may be described by the diffusion coefficients  $D_{||} \approx 8.47 \times 10^{-12} \text{ m}^2 \text{ s}^{-1}$  and  $D_{\perp} \approx 5.75 \times 10^{-12} \text{ m}^2 \text{ s}^{-1}$ , respectively (measured for the Perylene Diimide in 5CB by using NMR<sup>10</sup> technique), see also hereafter. In our case, the diffusion of chiral molecules is performed through planes with alternating direction of  $\mathbf{n}$  (Fig. 4) and, in addition, through multiple disclination zones. Thus, in the current work, we can only try to estimate the corresponding value of an effective diffusion coefficient  $D_e$ .

We further use the colored zones (the position of disclination walls representing a given value of  $C$ ) and their spatio-temporal changes as well as Fick's diffusion model<sup>4</sup> to roughly estimate the diffusion coefficient of our chiral molecules. To exclude the errors generated by the possible presence of meniscus between zone boundaries, we use (in our estimations) the colored zones, which have noticeably larger width compared to the thickness of our cell ( $d > L = 8 \mu\text{m}$ ). A simple case of diffusion with time  $t$  in one dimension ( $X$ -axis) from a starting point located at position  $x = 0$  (at the boundary of chiral liquid's droplet where the concentration is maintained at a given value  $C = C_0$  for  $x < 0$ ;  $C = 0$  for  $x > 0$  and  $t = 0$ ) may be represented as

$$C(x, t) \approx \frac{1}{2} C_0 \operatorname{erfc} \left( \frac{x}{2\sqrt{D_e}t} \right)$$

By using this approach we can represent the effective diffusion coefficients  $D_e$  of our two sandwiches (with and without strong boundary conditions) as it is demonstrated in Fig. 5.

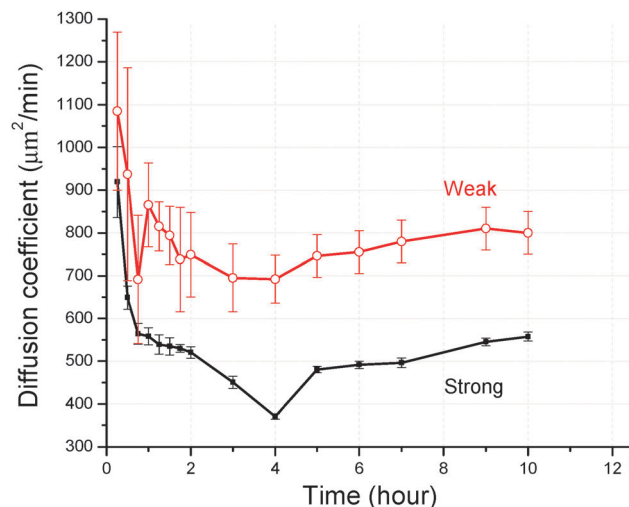


Fig. 5 Approximated estimation of the chiral molecules' dynamic diffusion coefficient in anisotropic host with and without strong boundary alignment conditions.

As we can see, the obtained effective diffusion coefficients are quite different for the two cases, when the host can freely adjust the orientation of its molecules (weak boundary condition) and when the host environment is rigidly aligned (strong boundary condition).

In reality, we have to mention that the orientational disclinations are relatively slow to adjust themselves; they are usually naturally resorbed in approximately few tens of minutes in standard cells of  $L = 8 \mu\text{m}$  thickness. This means that the disclination walls (between twisted zones of different pitch) may not necessarily follow (adapt themselves to) the *instantaneous* values of  $C(x)$ . The best way to insure the dynamic correlation (between the  $C(x)$  and the twist structure) would be the use of fluorescent dopants having non-zero twisting power and good miscibility with our NLC host.<sup>27</sup> It is not obvious, but we shall try to find such molecules for more quantitative comparisons in a future work.

In the meantime, to qualitatively validate our preliminary hypothesis, we have performed measurements of the diffusion of non-chiral dye molecules (with negligible twisting power) in the same NLC host. The cell preparation was made according to the procedure described before (strong anchoring was used here). The droplet of the chiral dopant was replaced by a small quantity of Azobenzene liquid crystal 572 (from Beamco), absorbing in the blue spectral region. Light transmission (through the cell) pictures were recorded using a simple microscope. The obtained results are presented in the Fig. 6. First, as expected, there is no director twisting and there are no distinct coloration zones (the yellow color in the inset is defined by the blue absorption of the dye; thus, higher is the dye concentration lower is the transmitted light intensity). Second, the diffusion of the dye is anisotropic (stronger in the direction of rubbing, identified in the inset by the vertical arrow, which has approximately a length of 6 mm). For example, the histograms of pixel intensity, recorded at  $t = 4$  hours (left picture of the inset)

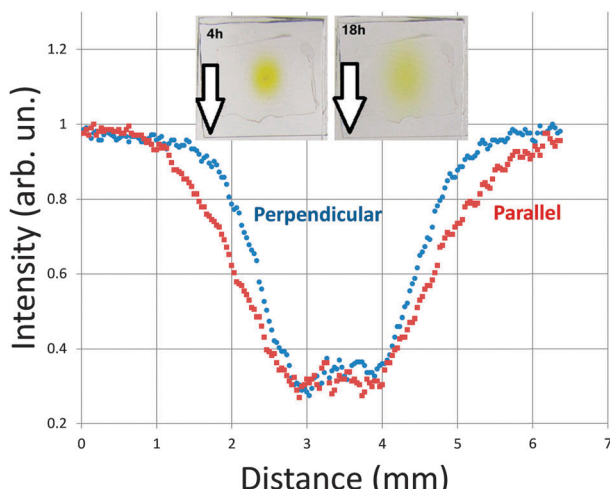


Fig. 6 Histograms obtained from the image recorded at  $t = 4\text{ h}$  (shown on the left of the inset) in parallel (squares) and perpendicular (circles) directions with respect to the rubbing direction (shown by the arrow in the inset) of the NLC doped by an achiral azobenzene dye.

in parallel with NLC's director (squares) and in perpendicular (circles) directions clearly show this anisotropy. The ratio of the corresponding half widths at half maximum (HWHM) is approximately  $\text{HWHM}_{\parallel}/\text{HWHM}_{\perp} \approx 1.4/1.1 \approx 1.27$  (at  $t = 4\text{ h}$ ). Thus, at the beginning, the diffusion process of azo dyes is relatively fast ( $\approx 1.4\text{ mm}/4\text{ h} = 0.35\text{ mm h}^{-1}$ ). This process is slowed down for longer time scales. Indeed, the right picture of the inset (recorded at 18 hours) still shows the anisotropic nature of diffusion, but also shows its slowing down:  $[\text{HWHM}_{\parallel}(18\text{ h}) - \text{HWHM}_{\parallel}(4\text{ h})]/[18 - 4]\text{ h} \approx 0.036\text{ mm h}^{-1}$ .

Obviously, this specific azo dye will diffuse differently from our chiral dopant for many reasons (because of the absence of elastic deformations; thanks to its liquid crystalline character, etc.). However, if we compare the progression of the discrete zones (from our microscope observations) in the case of the chiral dopant, we find a typical speed of disclination wall progression at the order of  $0.5\text{ mm h}^{-1}$  during the first 1 hour and another  $1\text{ mm}$  during the next 5 hours (thus  $\approx 1\text{ mm}/5 = 0.2\text{ mm h}^{-1}$ ). So in the time interval around 4–6 hours, the progression of disclination walls is slower, but not by orders of magnitude (only by a factor  $0.35/0.2 = 1.75$ ).

Keeping the above mentioned in mind and taking into account that our observations are done at larger time scales (compared to typical disclination resorption times) we think that our estimations of orders of magnitudes could be acceptable at the present level of qualitative analyses. Indeed, interestingly enough, despite the rough theoretical approximations, made here in the experimental data processing stage, the obtained typical (at  $\approx 1$  hour) diffusion coefficients ( $D_{e,\text{strong}} \approx 8 \times 10^{-12}\text{ m}^2\text{ s}^{-1}$  and  $D_{e,\text{weak}} \approx 13 \times 10^{-12}\text{ m}^2\text{ s}^{-1}$ ) seem to have rather reasonable order of magnitude. Most importantly, we would like to emphasize that our main goal in the present work is to show the difference of diffusion for strong and weak boundary conditions that appears to be rather significant ( $\approx 1.6$ ).

## Conclusions

Our experimental observations show a clear difference of diffusion of chiral molecules in an anisotropic media depending upon its orientational flexibility. Namely, the diffusion is stronger (by a factor of  $\approx 1.6$ ) if the host can easily adjust the overall alignment of its molecular orientation. Thus, the orientational rigidity of the host (its boundary conditions) can influence the diffusion of chiral molecules and we can control this process by the control of system's parameters (twisting power of the dopant, elastic deformation constant of the host, boundary conditions, orientational structure, temperature, etc.). To the best of our knowledge this is the first report of such "coupling" between the microscopic molecular diffusion and the collective (quasi macroscopic) elastic properties of the host offering a new insight of formation of molecular self-assemblies and also the exciting possibility of controlling the diffusion process in such material systems. Obviously, a significant amount of research must yet be performed to further study these processes. However, we can already imagine the important impact of our observations on diffusion processes of chiral species, for example, during the propagation of chirality in enantiomeric DNA,<sup>25</sup> the diffusion of cholesterol molecules into the myelin membranes,<sup>26</sup> etc. Based on our observations, we might also predict that the simultaneous propagation (diffusion) of a mixture of two chiral dopants (for example, a drug molecule and another molecule with the opposed twisting power, but not necessarily with the same chemical structure) in such media should be easier than the diffusion of the individual enantiomer of a given chirality since the twisting power of this mixture would be zero.

We would like to thank NSERC and the Canada Research Chair in Liquid Crystals and Behavioral Biophotonics as well as the Manning Innovation Award for the financial support of this project.

## Notes and references

- 1 A. N. Lien, H. Hu and P.-H. Chuong, Chiral Drugs: An Overview, *Int. J. Biomed. Sci.*, 2006, 2(2), 85–100.
- 2 Y. Bae, S. Fukushima, A. Harada and K. Kataoka, Design of Environment-Sensitive Supramolecular Assemblies for Intracellular Drug Delivery: Polymeric Micelles that are Responsive to Intracellular pH Change, *Angew. Chem., Int. Ed.*, 2003, 42, 4640–4643.
- 3 Y. Zhao, Rational Design of Light-Controllable Polymer Micelles, *Chem. Rec.*, 2007, 7, 286–294.
- 4 J. Crank, *The mathematics of diffusion*, Clarendon Press, Oxford University Press, Oxford, 1975.
- 5 P. G. De Gennes and J. Prost, *The Physics of Liquid Crystals*, Clarendon Press, 1995.
- 6 V. Tuchin, *Tissue Optics: Light Scattering Methods and Instruments for Medical Diagnosis*, SPIE press, Bellingham, Washington, 2nd edn, 2007.
- 7 C. Hoppmann, C. Barucker, D. Lorenz, G. Multhaup and M. Beyermann, Light-Controlled Toxicity of Engineered Amyloid b-Peptides, *ChemBioChem*, 2012, 13, 2657–2660.

- 8 S. Bassene and T. V. Galstian, Electrical Modulation of Coherent Scattering in Dual Frequency Liquid Crystal Tissue Models, *Mol. Cryst. Liq. Cryst.*, 2010, **526**(1), 58–68.
- 9 G. Celebre, G. De Luca, M. Maiorino, F. Iemma, A. Ferrarini, S. Pieraccini and G. P. Spada, Solute-Solvent Interactions and Chiral Induction in Liquid Crystals, *J. Am. Chem. Soc.*, 2005, **127**, 11736–11744.
- 10 M. Pumpa and F. Cichos, Slow Single-Molecule Diffusion in Liquid Crystals, *J. Phys. Chem. B*, 2012, **116**, 14487–14493.
- 11 T. Turiv, I. Lazo, A. Brodin, B. I. Lev, V. Reiffenrath, V. G. Nazarenko and O. D. Lavrentovich, Effect of Collective Molecular Reorientations on Brownian Motion of Colloids in Nematic Liquid Crystal, *Science*, 2013, **342**, 1351–1353.
- 12 I. I. Smalyukh, J. Butler, J. D. Shroud, M. R. Parsek and G. C. L. Wong, Elasticity-mediated nematiclike bacterial organization in model extracellular DNA matrix, *Phys. Rev. E: Stat., Nonlinear, Soft Matter Phys.*, 2008, **78**(3), 030701.
- 13 A. Kumar, T. Galstian, S. K. Pattanayek and S. Rainville, The Motility of Bacteria in an Anisotropic Liquid Environment, *Mol. Cryst. Liq. Cryst.*, 2013, **574**(1), 33–39.
- 14 S. Zhou, A. Sokolov, O. D. Lavrentovich and I. S. Aranson, Living liquid crystals, *Proc. Natl. Acad. Sci. U. S. A.*, 2014, **111**(4), 1265–1270.
- 15 P. C. Mushenheim, R. R. Trivedi, H. H. Tuson, D. B. Weibel and N. L. Abbott, Dynamic self-assembly of motile bacteria in liquid crystals, *Soft Matter*, 2013, **10**(1), 88–95.
- 16 P. C. Mushenheim, R. R. Trivedi, D. B. Weibel and N. L. Abbott, Using Liquid Crystals to Reveal How Mechanical Anisotropy Changes Interfacial Behaviors of Motile Bacteria, *Biophys. J.*, 2014, **107**(1), 255–265.
- 17 I. Duchesne, T. Galstian and S. Rainville, The anisotropic viscosity of DSCG solutions and its influence on the motility of bacteria, *Biophys. J.*, submitted.
- 18 K. Takatoh, M. Hasegawa, M. Koden, N. Itoh, R. Hasegawa and M. Sakamoto, *Alignment technologies and applications of liquid crystal devices*, Taylor & Francis, Abingdon & New York, 2005.
- 19 W. Zhao, C.-X. Wu and M. Iwamoto, Weak boundary anchoring, twisted nematic effect, and homeotropic to twisted-planar transition, *Phys. Rev. E: Stat., Nonlinear, Soft Matter Phys.*, 2002, **65**, 031709.
- 20 R. Cano, *Bull. Soc. Fr. Mineral. Cristallogr.*, 1969, **90**, 333.
- 21 H. de Vries, *Acta Crystallogr.*, 1951, **4**, 219.
- 22 C. Oseen, *Trans. Faraday Soc.*, 1933, **29**, 833.
- 23 K. Allahverdyan and T. Galstian, Electrooptic jumps in natural helicoidal photonic bandgap structures, *Opt. Express*, 2011, **19**(5), 4611.
- 24 O. D. Lavrentovich and D.-K. Yang, Cholesteric cellular patterns with electric-field-controlled line tension, *Phys. Rev. E: Stat. Phys., Plasmas, Fluids, Relat. Interdiscip. Top.*, 1998, **57**(6), R6269–R6272.
- 25 M. Rossi, G. Zanchetta, S. Klussmann, N. A. Clark and T. Bellini, Propagation of Chirality in Mixtures of Natural and Enantiomeric DNA Oligomers, *Phys. Rev. Lett.*, 2013, **110**, 107801.
- 26 G. Saher, B. Brugger, C. Lappe-Siefke, W. Möbius, R.-I. Tozawa, M. C. Wehr, F. Wieland, S. Ishibashi and K.-A. Nave, High cholesterol level is essential for the myelin membrane growth, *Nat. Neurosci.*, 2005, **8**(4), 468.
- 27 We thank the referee for this suggestion.